

Available online at [www.sciencedirect.com](http://www.sciencedirect.com)

ScienceDirect

journal homepage: [www.intl.elsevierhealth.com/journals/dema](http://www.intl.elsevierhealth.com/journals/dema)

## Survival of implant-supported resin-matrix ceramic crowns: *In silico* and fatigue analyses

Edmara T.P. Bergamo<sup>a,\*</sup>, Satoshi Yamaguchi<sup>b</sup>, Paulo G. Coelho<sup>c</sup>,  
Adolfo C.O. Lopes<sup>a</sup>, Chunwoo Lee<sup>b</sup>, Gerson Bonfante<sup>a</sup>,  
Ernesto B. Benalcázar Jalkh<sup>a</sup>, Everardo N.S. de Araujo-Júnior<sup>a</sup>,  
Estevam A. Bonfante<sup>a</sup>

<sup>a</sup> Department of Prosthodontics and Periodontology, University of São Paulo, Bauru School of Dentistry, 9-75, Otávio Pinheiro Brisola, 17012-901, Bauru, SP, Brazil

<sup>b</sup> Department of Biomaterials Science, Osaka University Graduate School of Dentistry, 1-8 Yamadaoka, 565-0871, Suita, Osaka, Japan

<sup>c</sup> Department of Biomaterials and Biomimetics, Hansjorg Wyss Department of Plastic Surgery, Mechanical and Aerospace Engineering, New York University, 345 24th Street, 10010, New York City, NY, USA

### ARTICLE INFO

#### Article history:

Received 3 July 2020

Received in revised form

20 October 2020

Accepted 30 December 2020

Available online xxx

#### Keywords:

Ceramics

Dental implants

Fatigue

Reliability

Weibull

### ABSTRACT

**Objective.** To evaluate the fatigue survival, failure mode, and maximum principal stress (MP Stress) and strain (MP Strain) of resin-matrix ceramic systems used for implant-supported crowns.

**Methods.** Identical molar crowns were milled using four resin-matrix ceramics (n = 21/material): (i) Shofu Hard, (ii) Cerasmart (iii) Enamic, and (iv) Shofu HC. Crowns were cemented on the abutments, and the assembly underwent step-stress accelerated-life testing. Use level probability Weibull curves at 300 N were plotted and the reliability at 300, 500 and 800 N was calculated for a mission of 50,000 cycles. Fractographic analysis was performed using stereomicroscope and scanning electron microscope. MP Stress and MP Strain were determined by finite element analysis.

**Results.** While fatigue dictated failures for Cerasmart ( $\beta > 1$ ), material strength controlled Shofu Hard, Enamic, and Shofu HC failures ( $\beta < 1$ ). Shofu HC presented lower reliability at 300 N (79%) and 500 N (59%) than other systems (>90%), statistically different at 500 N. Enamic (57%) exhibited a significant reduction in the probability of survival at 800 N, significantly lower than Shofu Hard and Cerasmart; however, higher than Shofu HC (12%). Shofu Hard and Cerasmart (>93%) demonstrated no significant difference for any calculated mission (300–800 N). Failure mode predominantly involved resin-matrix ceramic fracture originated from occlusal cracks, corroborating with the MP Stress and Strain location, propagating through the proximal and cervical margins.

**Significance.** All resin-matrix ceramics crowns demonstrated high probability of survival in a physiological molar load, whereas Shofu Hard and Cerasmart outperformed Enamic and Shofu HC at higher loads. Material fracture comprised the main failure mode.

© 2021 The Academy of Dental Materials. Published by Elsevier Inc. All rights reserved.

\* Corresponding author.

E-mail address: [edmarabergamo@usp.br](mailto:edmarabergamo@usp.br) (E.T.P. Bergamo).

<https://doi.org/10.1016/j.dental.2020.12.009>

10109-5641/© 2021 The Academy of Dental Materials. Published by Elsevier Inc. All rights reserved.

## 1. Introduction

All-ceramic alternatives for implant-supported crowns indicate an increasing use of porcelain-fused to zirconia (PFZ), as a substitute for metal ceramics, accounting for approximately 90% survival rates after 5 years in function [1–4]. Although such survival rates are high in the medium-term, a veneering ceramic chipping frequency of 24.5% for PFZ when compared to 9.5% for metal ceramics after 2.1 years has been observed [3]. Improvements in the mechanical performance have been reported in a study that found a chipping rate of 4% for PFZ and no failures for metal ceramics [2]. Veneering porcelain fracture in PFZ has been strongly associated with lower porcelain fracture toughness [5], deleterious residual stresses during the cooling phase of veneer sintering [6], among other causes. Also, when PFZ reconstructions are implant-supported, they may be more prone to fracture due to the lack of resiliency given by the periodontal ligament and its dampening effect upon occlusal forces [7,8]. Whereas results for tooth-supported reconstructions seem to be more encouraging, those for implant-supported crowns are still challenging and PFZ use has been suggested as a risk factor for failure, especially in the presence of an opposing ceramic reconstruction [9,10]. To overcome the aforementioned limitations, the development of monolithic blocks for computer-aided design/ computer-aided manufacturing (CAD/CAM) has become a fast-growing research field in the restorative arena [11].

New polymeric restorative systems highly filled with ceramics are available through discs and/or blocks for milling and incorporate innovations in materials composition and microstructure [11–14]. The so-called resin-matrix ceramic systems are usually comprised of methacrylate-based polymer matrices containing predominantly inorganic compounds that might include glasses, porcelains, glass-ceramics, and ceramics, and have been coded as ceramics by the American Dental Association (ADA) due to their high ceramic content [11,14–16]. Despite the ADA designation, materials science is very clear in defining such composites as polymer systems [14,17]. Advantages of these materials include a homogeneous, dense, and reliable microstructure due to block/disc fabrication under an industrial environment in high temperature and pressure [18,19], as well as milling damage tolerance that may be linked to an excellent machinability and small marginal gap, no need for post-milling firing, easy adjustment and polishing for optimal occlusion, and reparability [11,13]. The mechanical properties of different resin-matrix ceramic systems are dictated by their composition and microstructure, presenting a range of 150–270 MPa in flexural strength and 10–30 GPa in elastic modulus [11,13,20,21].

The improved biomechanical behavior of resin-matrix ceramics for implant-supported reconstructions is determined by their polymeric content and lower elastic modulus relative to ceramics, likely providing favorable resilience and improving occlusal forces dampening and damage tolerance [22–27]. In the implant-supported scenario, reconstructions with resin-matrix ceramics have been associated with significantly reduced stress transmission to the peri-implant

area, which may also decrease long-term biological complications [22,23]. Despite favorable biomechanics, a recent systematic review and meta-analysis comparing the clinical performance of implant-supported single crowns has exhibited a high fracture rate for a first-generation resin-matrix ceramic system (33% after 5 years), which was statistically higher compared to all-ceramic systems such as lithium disilicate and zirconia (both ~9%) [4]. Apparently, the material composition negatively influenced its fracture stability in a demanding functional scenario, thus modifications in the filler compounds and weight content and microstructure of newly developed resin-matrix systems claiming to expand clinical application, especially for implant reconstructions, have been proposed and demand further investigations.

Restorative systems placed in the oral cavity interact with the oral environment and a complex chemically assisted mechanical scenario operate in the damage initiation and propagation through slow crack growth that leads to a reduction in strength [28,29]. Therefore, fatigue testing has been considered a clinically relevant predictor of materials resistance to environmentally assisted functional damage [29,30]. However, there is scarce information about the fatigue properties of several resin-matrix ceramics milled in anatomical geometries [27,31–33]. Hence, this study evaluated the probability of survival, failure modes and maximum principal stress (MP Stress) and strain (MP Strain) of implant-supported molar crowns of different resin-matrix ceramic systems when subjected to step-stress accelerated-life fatigue testing. The postulated null hypotheses were: (i) that resin-matrix ceramic systems would not present different fatigue survival, (ii) that resin-matrix ceramic systems would not present different fatigue failure mode, and (iii) that resin-matrix ceramic systems would not present substantially different MP Stress/Strain concentration and distribution.

## 2. Materials and methods

Eighty-four Ti-6Al-4V abutments for implants with a locking taper connection (Universal abutments, Bicon LLC, Boston, MA, USA) and implants (3 mm well, 8 mm height, Bicon LLC) were obtained. A wax model maxillary first molar crown was scanned (InEos Blue, Sirona, Charlotte, NC, USA) and crowns were milled (inLab MC XL, Sirona) from four hybrid ceramic systems blocks (n = 21/group) [13,20,21]:

- (i) Shofu Hard: fine-structured zirconium silicate and methacrylate monomers ( $\sigma$ : 270 MPa, E: ~10 GPa, Shofu Dental Corporation, Tokyo, Japan),
- (ii) Cerasmart: feldspathic ceramic and methacrylate monomers ( $\sigma$ : 230 MPa, E: ~10 GPa, GC Corporation, Tokyo, Japan),
- (iii) Enamic: feldspathic ceramic network and methacrylate monomers ( $\sigma$ : 150 MPa, E: 30 GPa, Vita Zahnfabrik, Bad Sackingen, Germany), and
- (iv) Shofu HC: zirconium silicate and methacrylate monomers ( $\sigma$ : 190 MPa, E: ~10 GPa, Shofu Dental Corporation).

Crowns were finished and polished according to manufacturers' instructions. A self-adhesive resin composite cement

(RelyX U200, 3M Oral Care, St. Paul, MN, USA) was used to bond the crowns, which had their cementation surface previously etched with 5% hydrofluoric acid for 60 s (Enamic and Cerasmart), or sandblasted with aluminum oxide 50  $\mu\text{m}$  particles with 0.2 MPa pressure for 10 s (Shofu Hard and Shofu HC) followed by cleaning with ethanol, and then treated with a layer of ceramic primer (RelyX Ceramic Primer, 3M Oral Care, MN). A crown/implant positioning apparatus was fabricated to allow repeated pouring of the self-curing acrylic resin (Orthodontic Resin, Dentsply-Caulk, Philadelphia, PA, USA) and standardized embedding of samples to be fixed on the testing machine.

### 2.1. Step-stress accelerated life testing (SSALT) and reliability analysis

SSALT was performed in an axial direction at constant frequency of 10 Hz with the spherical indenter (6 mm diameter, D-2 Steel) positioned at the mesiolingual cusp (ElectroPuls™ E3000 Linear-Torsion system mechanical testing equipment, Instron, Norwood, MA, USA). Crowns were submerged in water at room temperature throughout fatigue testing. Although details of SSALT method used in this study has been described elsewhere [30,32–36], in brief, three profiles were designed as mild, moderate, and aggressive, with the number of specimens assigned to each group being distributed in the ratio of 3:2:1, respectively ( $n = 9$  in the mild,  $n = 6$  in the moderate, and  $n = 3$  in the aggressive load profile). These profiles are named based on the step-wise load increase that the specimen will be fatigued throughout the cycles until a certain level of load, meaning that specimens assigned to a mild profile will be cycled longer to reach the same load level of a specimen assigned to the aggressive profile [30]. Fatigue loads throughout SSALT ranged from 200 N up to a maximum of 2000 N with a steady increase in load as a function of elapsed cycles. The test was conducted until specimen failure or suspension (absence of fracture until the end of a profile). The findings were recorded as fracture load, number of cycles in which the sample failed, and stress profile.

Data analysis consisted of an underlying life distribution that described the life data collected at different stress levels and a life-stress model that quantified the manner in which the life distribution changed across different stress levels [33,34,37]. Thus, the Weibull Distribution was chosen to fit the life data collected in SSALT. Considering the time-varying stress model of SSALT, the inverse power law relationship was selected to extrapolate a use level condition considering the cumulative effect of the applied stresses, commonly referred as the cumulative damage model. From the extrapolated use level condition, a variety of functions could be derived. Hence, the use level probability Weibull curves (probability of failure versus number of cycles) with a set load of 300 N at 90% two-sided confidence interval were calculated and plotted (CI: 90%) (Synthesis 9, Alta Pro, Reliasoft, Tucson, AZ, USA). Also, the reliability was calculated for completion of a mission of 50,000 cycles at 300, 500, and 800 N and the differences between groups were identified based on the non-overlap of the CI. Parameters estimation was accomplished via maximum likelihood estimation (MLE)

**Table 1 – Properties of the resin-matrix ceramic systems used for finite element analysis.**

	Elastic modulus (MPa)	Poisson ratio
Shofu Hard	8,800	0.38
Cerasmart	7,300	0.38
Enamic	15,000	0.38
Shofu HC	6,000	0.38
Abutment	114,000	0.34
Cement	8,000	0.33

method, and CI were approximated using the Fisher matrix approach.

If the calculated use level probability Weibull beta parameter of any group was  $<1$ , then a Weibull 2-parameter calculation of the Weibull modulus, a unitless parameter that measures the variability of the results, and the characteristic strength, load at which 63.2% of the specimens would fail, was presented using the final load failure or survival (Weibull 9++, Reliasoft) [33,34,37]. Weibull 2-parameter contour plot (Weibull modulus vs. characteristic strength) was graphed to determine statistical differences through the non-overlap of CI. Parameters estimation was accomplished via MLE method, and 90% CI were approximated using the Fisher matrix approach.

### 2.2. Fractographic analysis

Failed samples were first inspected in polarized light stereomicroscope (AxioZoom V16, Zeiss, Oberkochen, Germany) using Z-stack capture mode which uses automated sequential imaging along the z-plane and sticks them within the same depth of focus (ZEN 2.3 PRO, Zeiss) to depict fracture planes and allow fractographic analysis under magnifications up to 260 $\times$ . Subsequently, fractured samples were evaluated under scanning electron microscope (SEM, Model 3500S, Hitachi Ltd., Osaka, Japan). Criteria used for failure were cohesive fracture within the composite (chipping), fracture exposing the abutment or fracture in several pieces (catastrophic), and abutment fracture.

### 2.3. In silico voxel based finite element analysis (FEA)

Each stereo lithography (STL) file scanned was voxelized with 0.05 mm/voxel in the voxel based FEA software (VOXELCON2015, Quint, Fuchu, Japan). Total voxel number was 5,880,870. Elastic modulus of each material was summarized in Table 1. Poisson's ratio of each material was set to 0.38 according to that of dental composites [38]. Z axes for FEA models were defined along axial direction. Static loads of 300 N, 500 N, and 800 N were loaded on an area according to loading condition of *in vitro* fatigue testing as shown in Fig. 1. CAD/CAM resin-matrix ceramic crowns were perfectly cemented on the abutment and the bottom surface of the abutment was completely fixed along to X, Y, and Z axes. By following aforementioned boundary conditions, the voxel based FEA was conducted using matrix solver with an error of 0.0001 [39]. Maximum principal stress (MP Stress) and strain (MP Strain) distribution were assessed, and maximum values were compared.

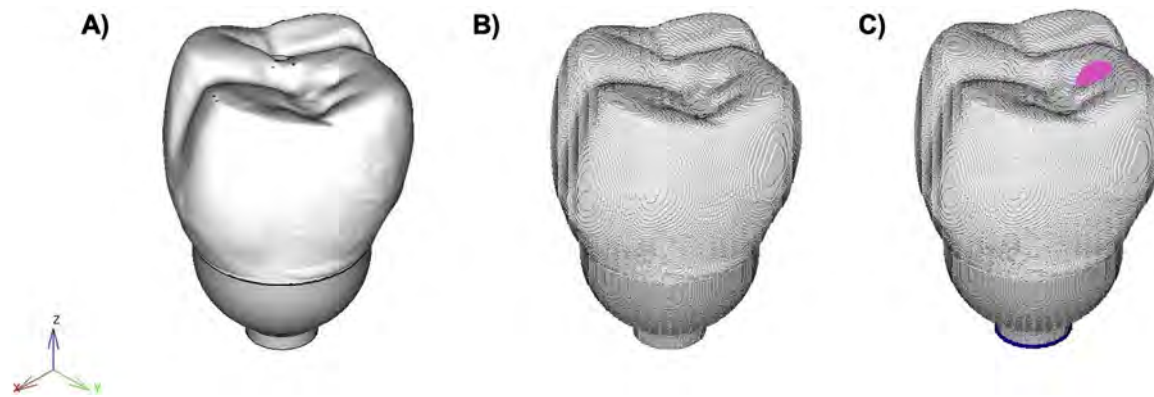


**Fig. 1** – CAD model of implant-supported crown used for finite element analysis (FEA) (A), where the stl. file was voxelized with 0.05 mm/voxel in the FEA software (B). Loading condition was based on the fatigue test settings, with indentation area near the cusp tip and the central fossa (C).

**Table 2** – Probability of Survival (%) and the respective 90% confidence interval for an estimated mission of 50,000 cycles at 300, 500, and 800 N.

		Shofu Hard	Cerasmart	Enamic	Shofu HC
300 N	Upper Bound	100	99	99	89
	Reliability	98 aA	96 aA	97 aA	79 aA
	Lower Bound	89	88	88	64
500 N	Upper Bound	99	99	96	71
	Reliability	97 aA	96 aA	90 aA	59 bA
	Lower Bound	86	86	76	39
800 N	Upper Bound	98	99	72	26
	Reliability	93 aA	96 aA	57 bB	12 cB
	Lower Bound	80	80	38	4

Different lowercase letters indicate statistically significant difference between materials. Different uppercase letter indicates statistically significant difference between missions.

### 3. Results

The calculated probability of survival for completion of a mission of 50,000 cycles at 300, 500, and 800 N is presented in the Table 2. All CAD/CAM hybrid ceramic systems presented no significant difference on the probability of survival at 300 N, although Shofu HC showed notably lower values (79%) than the others (more than 96%). While Shofu Hard, Cerasmart and Enamic crowns kept their survivability higher than 90% at a set load of 500 N, a significantly reduced reliability was demonstrated by Shofu HC crowns (59%). Similarly, the cumulative damage reaching a high-magnitude mission (800 N) would result in significantly reduced reliability to Shofu HC (12%), as well as Enamic (57%) crowns, both significantly different between them. Indeed, Shofu Hard and Cerasmart implant-supported crowns demonstrated no significant difference for all calculated missions corresponding to molar forces range (300–800 N), and both systems maintained the probability of survival higher than 93%.

Use level probability Weibull curves at a use level load of 300 N for all tested resin-matrix ceramic systems are shown in Fig. 2. The Beta values ( $\beta$ ) derived from use level probability Weibull parameters calculation were lower than 1 for Shofu HC ( $\beta$ : 0.23 CI: 0.13–0.40), Enamic ( $\beta$ : 0.29 CI: 0.13–0.61) and Shofu Hard ( $\beta$ : 0.72 CI: 0.18–2.89), which indicate strength

as the main factor dictating failure behavior, whereas Cerasmart ( $\beta$ : 3.52 CI: 2.20–5.56) beta values were higher than 1 and damage accumulation as a consequence of fatigue dictated failures. Nonetheless, Shofu Hard confidence interval upper bounds also indicated the influence of fatigue damage accumulation on failure rate. The Weibull 2-parameter contour plot (Weibull modulus vs. characteristic strength), presented in Fig. 3, shows that the Weibull modulus was similar between groups (2.7–4.4), whereas the characteristic strength considering load at failure during fatigue was significantly higher for Shofu Hard (2000 N) and Cerasmart (1539 N) when compared to Enamic (1014 N) and Shofu HC (754 N), both significantly different between them.

The failure modes were mainly confined to the resin-matrix ceramic materials and involved cohesive fractures (chipping), ceramic fracture with abutment exposure or fracture in several pieces (catastrophic) (Figs. 4–6). Some samples failing approximately at 2000 N under fatigue in the Shofu Hard group presented abutment fracture (Fig. 7). Nonetheless, chipping and delamination were the most frequently observed event. Eight crowns for Shofu Hard, 3 crowns for Cerasmart and 1 for Enamic were suspended due to profile completion without failure at approximately 2000 N.

A representative Shofu Hard suspended crown was sectioned for evaluation of the subsurface damage crack features. The micrographs demonstrated wear and contact damage

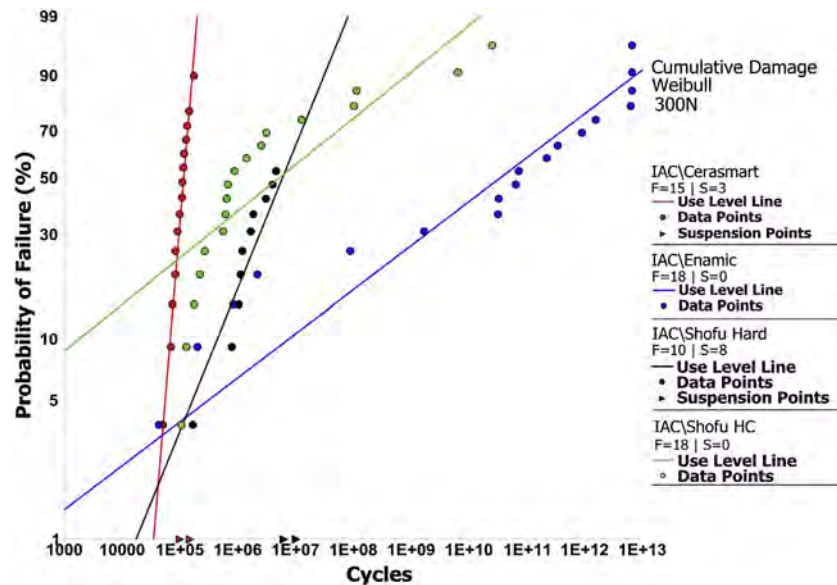


Fig. 2 – Use level probability Weibull curves evidencing the probability of failure as a function of elapsed cycles for polymeric implant-supported crowns at 300 N of set load.

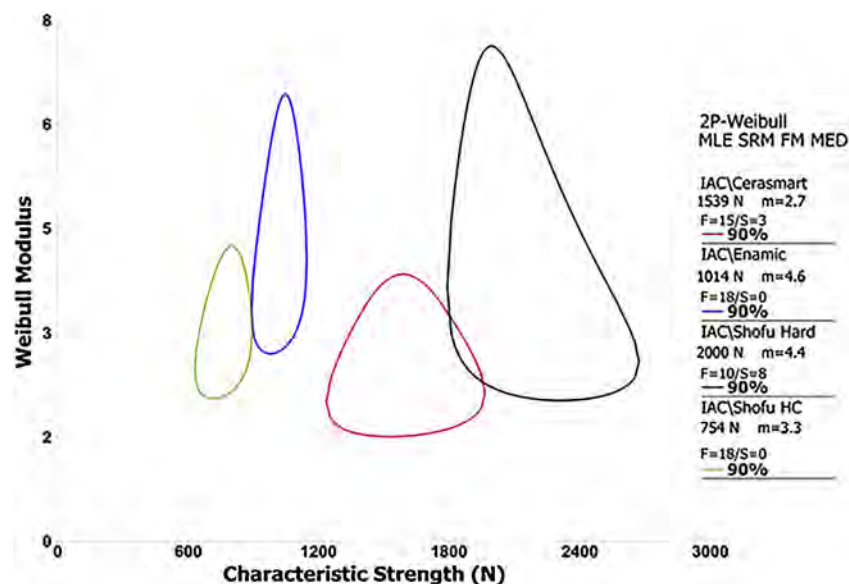


Fig. 3 – Contour plot evidencing the characteristic strength (N) and Weibull Modulus (m) of the polymeric implant-supported crowns. The non-overlap of the contours indicates statistically significant difference.

deformation under the loading area and the development of near-field occlusal contact cracks (inner cone cracks) (Fig. 4). Continued damage accumulation and microcracking at the indenter area resulting in inner cone crack deepening eventually led to crown fracture in different failure modes, as shown in Figs. 5 and 6. Cohesive fracture especially within Shofu HC and Enamic occurred at loads approximately of 600 N and invariably started from the occlusal indentation area, which led to subsurface damage and crack propagation towards the proximal and cervical margins of the restorations (Fig. 5). Shofu Hard and Cerasmart fracture mostly occurred at high loads (>1000 N) with several fracture origins, all starting from the indentation area to restorations margins that led final frac-

ture exposing the abutment, leaving telltale marks such as hackles, arrest lines, and twist hackles (Fig. 6).

Abutment failure occurred at very high loads (>1300 N) and the fracture initiated where the crown loading led to local tensile stress, at the abutment collar level, and propagated creating a plastic deformation zone as a result of titanium ductile behavior and a compression curl on the opposite side of the fracture origin (Fig. 7).

The maximum principal stress (MP Stress) and strain (MP Strain) were observed around the mesiolingual cusp for all resin-matrix ceramic systems and initiated by quasiplastic deformation under compression loading (Fig. 8), as indicated in vitro (Fig. 4B). The dominant tensile MP Stress was observed



**Fig. 4** – Stereomicroscope (A and A.1) micrographs of a cross-sectioned suspended crown showing the development of cone cracks (CC) under the loading area. SEM (B) image of the crown evidencing the contact damage and quasiplastic deformation on the loading area (asterisk).

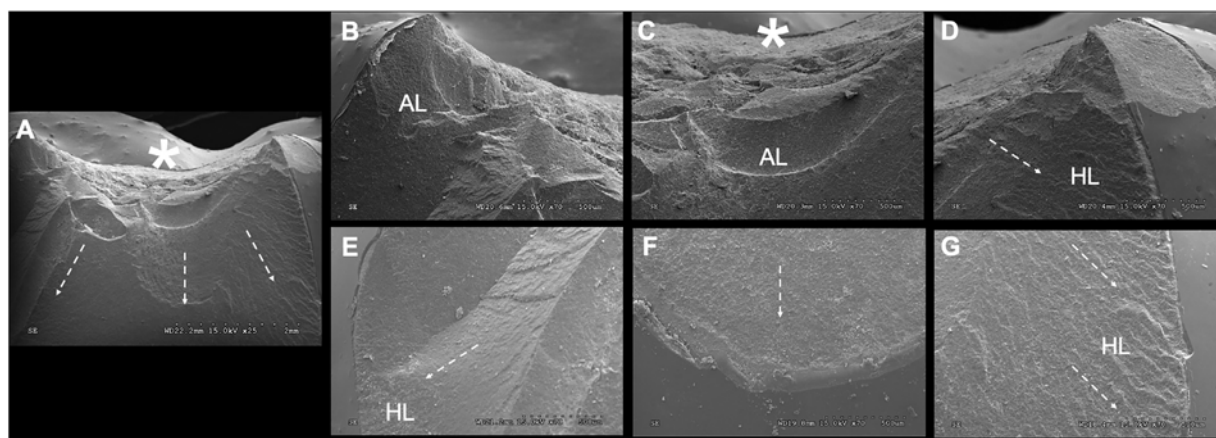


**Fig. 5** – SEM images of a fractured crown at a lower load and cohesive fracture of the ceramic material. The micrographs indicate the origin (\*) and the direction of crack propagation (white arrows), with the crack initiating under the loading surface and propagating all the way through the proximal and cervical margins. Fractographic marks support the direction of crack propagation by the presence of multiple hackle lines (HL) and arrest lines (AL).

**Table 3** – Maximum principal stress (MP Stress, MPa) and strain (MP Strain) values obtained in the finite element analysis under 300, 500, and 800 N.

		Shofu Hard			Cerasmart			Enamic			Shofu HC		
		300	500	800	300	500	800	300	500	800	300	500	800
Crown	MP Stress	128	213	341	130	217	347	128	213	342	128	213	341
	MP Strain	0.05	0.08	0.13	0.02	0.04	0.07	0.06	0.11	0.17	0.04	0.07	0.12
Abutment	MP Stress	399	665	1065	339	665	1064	399	665	1067	399	665	1064
	MP Strain	0.004	0.006	0.01	0.004	0.006	0.01	0.004	0.006	0.01	0.004	0.006	0.01
Cement	MP Stress	23	38	61	24	40	65	17	28	45	28	47	75
	MP Strain	0.006	0.01	0.01	0.004	0.007	0.01	0.007	0.01	0.02	0.006	0.01	0.015

around the abutment collar level of the buccal surface (Fig. 8a), as also indicated *in vitro* (Fig. 7). Both failure criteria indicated similar values for all resin-matrix ceramic systems after the voxel-based finite element analysis under 300 N, 500 N, and 800 N loadings, same range of load estimated in the reliability analysis (Table 3).

#### 4. Discussion

One rationale for the development of CAD/CAM resin-matrix ceramics lies on their lower elastic modulus relative to glass-ceramics or polycrystalline ceramics [11,20]. Such sys-

tems have been suggested to improve occlusal forces by dampening and reducing stress transmission to the peri-implant area and may be considered unique for implant supported-reconstructions considering that patients with implants have a decreased proprioception and lower tactile sensitivity [8,22,23]. In addition, resin-matrix ceramics are less prone to fracture during milling and are easier to adjust than most ceramics, and should repair or anatomy modification be required, direct or indirect resin composite may be handy [11,15,33]. Our results showed high probability of survival for all resin-matrix ceramics with a physiological occlusal load, whereas Shofu Hard and Cerasmart outperformed Enamic and Shofu HC (both significantly different)

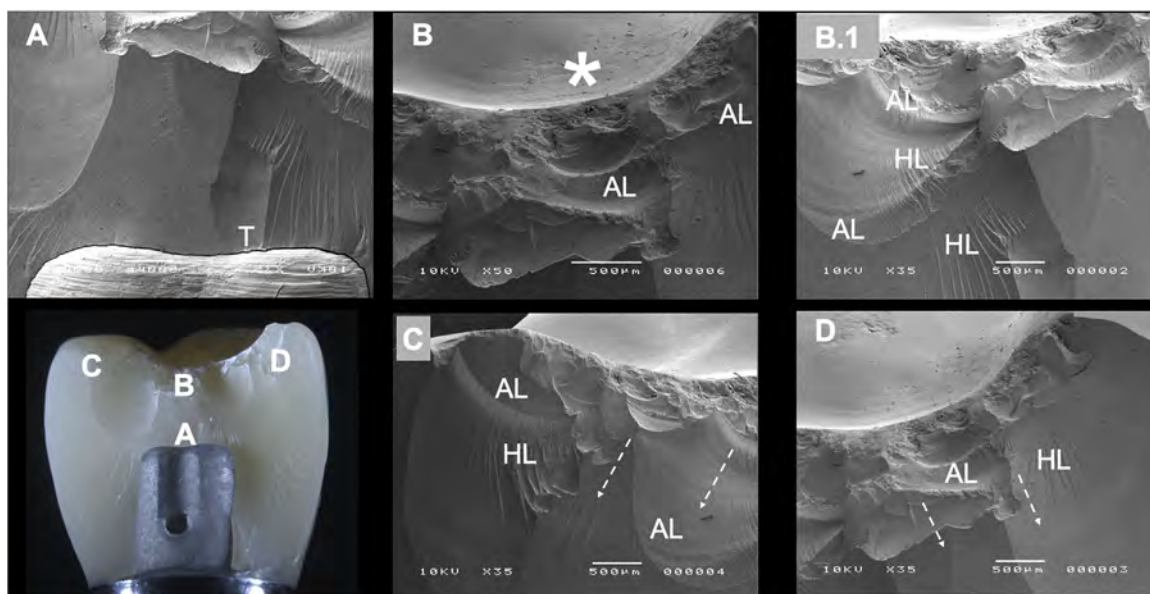


**Fig. 6 – SEM Micrographs of a fractured crown at a higher load with abutment exposure. The micrographs indicate the origin (\*) and the direction of crack propagation (white arrows). The SEM images indicate that cracks originated under the loading surface propagated all the way through the proximal and cervical margins. Fractographic marks support the direction of crack propagation by the presence of multiple hackles (H), arrest lines (AL), and twist hackles (T).**

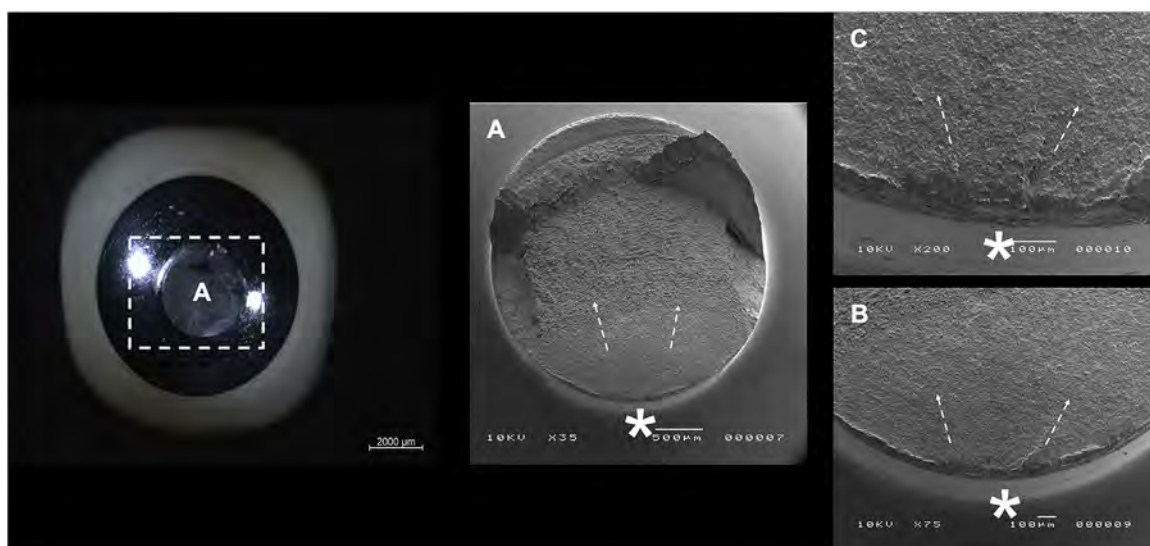


**Fig. 7 – SEM micrographs of a representative fractured abutment indicate the origin (\*) and the direction of crack propagation (white arrows). The fracture initiates where the crown loading led to a local tensile stress, located in the abutment collar level of the buccal surface and propagated to the opposite side.**

at high-load missions, consequently the first postulated null hypotheses that resin-matrix ceramic systems would not present different fatigue survival was rejected. Also, resin-matrix ceramic cohesive fracture comprised the main failure mode for Enamic and Shofu HC, whereas chief crown fracture with abutment exposure and sometimes into several pieces were observed for Cerasmart and Shofu Hard, thus the second postulated hypothesis that resin-matrix ceramic systems would not present different fatigue failure mode was also rejected. Finally, no substantial MP Stress and MP Strain

differences were observed between groups, then the third postulated hypothesis that resin-matrix ceramic systems would not present substantially different MP Stress/Strain concentration and distribution was accepted.

Failure rate interpretation based on the use level probability Weibull parameters indicated that Shofu HC and Enamic performance was not affected by damage initiation as fatigue cycles elapsed since beta ( $\beta$ ) values were less than 1, which has been commonly associated with failures that occur at a relatively early time due to egregious flaws. In contrast, the fatigue

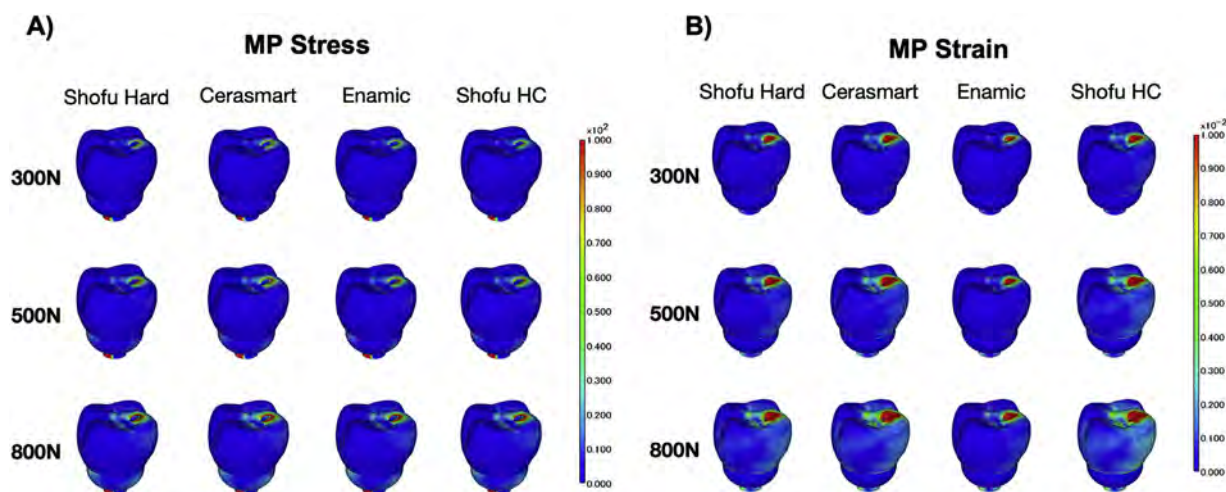


**Fig. 8 – Maximum principal stress (MP Stress) and strain (MP Strain) location on the crown, cement, and abutment under 300, 500, and 800 N.**

accelerated failures for Cerasmart as  $\beta$  values were higher than 1 and the cumulative damage triggered by the mechanical loading and environmentally assisted cracking dictated failure, which has been commonly associated with late failures [28,29,33,34,37]. Shofu Hard confidence interval bounds indicate a chief influence of materials strength, in this case at high loads; however, fatigue damage accumulation presence can also drive failure rate. Previous investigations under the same methodology have shown similar failure rates [18,32,33,35].

The survival was estimated based on the failure distribution by establishing a load range compatible with physiological occlusal loads and maximum bite forces reported for the molar region [40]. The reliability for completion of a 300 N load mission showed no significant difference for all resin-matrix ceramics. While Shofu HC (57%) and Enamic (59%) exhibited a statistically significant reduction in the probability of survival at higher loads (500 and 800 N, respectively), Shofu Hard and Cerasmart (>93%) demonstrated no significant difference for all calculated missions (300–800 N). Similarly, Weibull analysis considering the fatigue load at failure showed significantly higher values for Shofu Hard and Cerasmart, statistically superior to Enamic and Shofu HC (both significantly different, whereas all data have exceeded molar bite forces [40]. Given their similar composition and polymerization mode, resin-matrix ceramics differences in terms of fatigue resistance may be associated with their microstructure [12,14,25,41]. Size, distribution and weight content (wt%) of filler particles and its incorporation into the resin matrix may have influenced interfacial adhesion and presence of voids and defects, with systems composed of small particles and high filler content being mechanically advantageous [13,14,42,43]. Shofu Hard and Cerasmart has previously shown the presence of silica/zirconia nanoparticles and nanoclusters that favors the incorporation of a higher content of inorganic compounds (>70 wt%), while Shofu HC has exhibited lower inorganic content (~60 wt%) [14]. An important mechanism of polymer-based systems microstructural degradation may be related to soft matrix wear and exposure of the reinforcing ceramics to fracture and/or particles dislodgment, which may lead to crack

growth deeper into the material and, consequently decreased fatigue resistance [12,26]. A severe subsurface damage and volume loss have been reported for resin-matrix ceramics following a similar fatigue protocol, with systems composed of nanoparticles and nanoclusters resulting in small fragments break, i.e. Shofu Hard and Cerasmart [12]. Additionally, the method of polymer infiltration into a rigid ceramic network, i.e. Enamic system, has shown to originate microstructural defects in the boundary of the ceramic scaffold due to stresses generated by the resin matrix curing shrinkage, which may have also negatively affected its fatigue performance at high loads [14,42,43].

Despite their reported modest flexural strength, resin-matrix ceramics have shown higher damage tolerance due to lower brittleness when compared to conventional glass-ceramics, with approximately 60% less crack formation after fatigue testing [27]. Such a behavior was associated with their lower elastic modulus and higher energy absorption capacity, which also favors crack deflection toughening effect and increases R-curve behavior [25,27]. Particularly, discontinuous nanofilled systems (Shofu Hard and Cerasmart,  $E \sim 10$  GPa) instead of continuous ceramic network systems (Enamic,  $E:30$  GPa) have been associated with more favorable elastic-plastic deformation and impact absorption, raising the critical load for crack initiation by reducing the stress intensity at critical flaws [27]. The susceptibility to slow crack growth that dictates ceramic systems fatigue performance has also denoted lower coefficients for resin-matrix ceramics relative to glass-ceramics, resulting in a small difference when fast fracture and fatigue fracture were compared [41]. In fact, resin-matrix ceramics have shown a 15% decrease in strength compared to their initial fracture strength, which is half of the strength decrease observed for conventional glass-ceramics (32%) [26]. Previous data on fatigue survival of resin-matrix ceramic systems have also indicated a high survival for implant-supported crowns (>99% at 300 N), similar to metal ceramics [32]. Therefore, all the previously mentioned facts support the potential benefits of dispersed inorganic compounds as resin-matrix systems reinforcement, as well as the superior

performance of nanoparticles and nanoclusters in increasing their mechanical properties; however, such topics demand further investigation, especially concerning their clinical long-term performance [13,21].

Failures in restorative systems are usually originated from structural defects that arise either during manufacturing processes or functional use, as corroborated by the failure rate behavior of the different systems investigated in the current study and its effect on the final load at failure [29,30,32]. The observed failure modes in the current study were cohesive fracture within the ceramic material (chipping), fracture exposing the abutment or fracture in several pieces (catastrophic), and abutment fracture. However, cohesive fracture was mostly observed at lower loads and for failing samples from Enamic and Shofu HC groups. When loads increased, especially for Cerasmart and Shofu Hard, fractures were substantially larger leading to abutment exposure or to catastrophic failures or even in abutment fractures in samples almost reaching the end of the profile load of 2000 N. Nevertheless, irrespective of group, fractures originated from the indentation area and extended towards proximal and cervical margins of the crowns. Voxel-based finite element analysis (FEA) used in this study, which has previously shown to be adaptable to complex CAD models and effective to predict crack initiation of CAD/CAM polymeric crowns [44], corroborate with fractographic analysis findings, where the MP Stress and MP Strain were observed within mesiolingual cusp for all resin-matrix ceramic systems at functional molar loads [40]. As loads were increased, stress volumes and MP Stress at and below the surface also increased, corroborating with the larger number of catastrophic failures observed at higher loads.

From a clinical perspective, it is worth to mention that some of the observed fractures can be either repolished or repaired [11,33]. In chippings occurring under lower loads (~600 N, values within maximum voluntary bite forces [40]), and where the occlusal contacts were not affected, repolishing could return them to function, as done in a study evaluating implant-supported crowns restored with indirect resin-matrix system [45]. At higher loads (600–1300 N), fractures were commonly larger and might interfere with occlusal contacts but were still technically repairable. The intraoral repair of resin-matrix ceramic crowns can be performed by preconditioning, sandblasting, or bur roughening, followed by the placement of a direct or indirect resin composite [25,46]. A previous study has demonstrated that the reliability of implant-supported resin-matrix ceramic crowns is maintained after repair when compared to its intact counterpart, suggesting more favorable results than resin composite repair in glass-ceramics and polycrystalline ceramics [33].

Few abutment failures occurred from loads starting at 1300 N, suggesting that the friction-locking system of internal conical implant-abutment connection, which extends the contact of the abutment with the implant internal walls, favored prosthesis components biomechanics [45,47,48]. The choice for a tapered interference fit implant-abutment connection design, which is exempt from an abutment screw [45,48], was aimed at avoiding abutment screw fractures or even abutment fractures shown to occur at much lower load levels than those required for crown material failure [32,47].

Although randomized controlled trials provide the highest level of scientific evidence on implant and prosthesis performance, these studies must be preceded by laboratorial characterization of their physical and mechanical properties in a comparative manner as clinical trials are expensive and time-consuming [26,30]. The outcomes of the current study should not be directly extrapolated to in vivo conditions, but the findings suggest promising generations of resin-matrix ceramic materials that may provide a reliable treatment alternative, especially for implant-supported reconstructions where repair is commonly used to extend their lifetime.

## 5. Conclusion

All resin-matrix ceramics demonstrated high probability of survival, within physiological occlusal loads, whereas Shofu Hard and Cerasmart outperformed Enamic and Shofu HC at high-load missions. Resin-matrix ceramics fracture comprised the main failure mode.

## Acknowledgements

To Fundação de Amparo a Pesquisa do Estado de São Paulo (FAPESP) Young Investigators Award grant 2012/19078-7, EMU 2016/18818-8, FAPESP 2016/17793-1, 2019/08693-1, and to Conselho Nacional de Desenvolvimento Científico e Tecnológico (CNPq) grants # 304589/2017-9 and 434487/2018-0, and to CAPES Finance Code 001.

## REFERENCES

- [1] Pjetursson BE, Valente NA, Strasding M, Zwahlen M, Liu S, Sailer I. A systematic review of the survival and complication rates of zirconia-ceramic and metal-ceramic single crowns. *Clin Oral Implants Res* 2018;29(Suppl 16):199–214.
- [2] Hosseini M, Worsaae N, Schiodt M, Gotfredsen K. A 3-year prospective study of implant-supported, single-tooth restorations of all-ceramic and metal-ceramic materials in patients with tooth agenesis. *Clin Oral Implants Res* 2013;24:1078–87.
- [3] Schwarz S, Schroder C, Hassel A, Bomicke W, Rammelsberg P. Survival and chipping of zirconia-based and metal-ceramic implant-supported single crowns. *Clin Implant Dent Relat Res* 2012;14(Suppl 1):e119–25.
- [4] Rabel K, Spies BC, Pieralli S, Vach K, Kohal RJ. The clinical performance of all-ceramic implant-supported single crowns: a systematic review and meta-analysis. *Clin Oral Implants Res* 2018;29(Suppl 18):196–223.
- [5] Quinn JB, Quinn GD, Sundar V. Fracture toughness of veneering ceramics for fused to metal (PFM) and zirconia dental restorative materials. *J Res Natl Inst Stand Technol* 2010;115:343–52.
- [6] Kim J, Dhital S, Zhivago P, Kaizer MR, Zhang Y. Viscoelastic finite element analysis of residual stresses in porcelain-veneered zirconia dental crowns. *J Mech Behav Biomed Mater* 2018;82:202–9.
- [7] Pjetursson BE, Bragger U, Lang NP, Zwahlen M. Comparison of survival and complication rates of tooth-supported fixed dental prostheses (FDPs) and implant-supported FDPs and single crowns (SCs). *Clin Oral Implants Res* 2007;18(Suppl 3):97–113.

- [8] Meyer G, Fanghanel J, Proff P. Morphofunctional aspects of dental implants. *Ann Anat* 2012;194:190–4.
- [9] Koenig V, Vanheusden AJ, Le Goff SO, Mainjot AK. Clinical risk factors related to failures with zirconia-based restorations: an up to 9-year retrospective study. *J Dent* 2013;41:1164–74.
- [10] Pieralli S, Kohal RJ, Rabel K, von Stein-Lausnitz M, Vach K, Spies BC. Clinical outcomes of partial and full-arch all-ceramic implant-supported fixed dental prostheses. A systematic review and meta-analysis. *Clin Oral Implants Res* 2018;29(Suppl 18):224–36.
- [11] Ruse ND, Sadoun MJ. Resin-composite blocks for dental CAD/CAM applications. *J Dent Res* 2014;93:1232–4.
- [12] Wendler M, Kaizer MR, Belli R, Lohbauer U, Zhang Y. Sliding contact wear and subsurface damage of CAD/CAM materials against zirconia. *Dent Mater* 2020;36:387–401.
- [13] Lucsanzky IJR, Ruse ND. Fracture toughness, flexural strength, and flexural Modulus of new CAD/CAM resin composite blocks. *J Prosthodont* 2020;29:34–41.
- [14] Mainjot AK, Dupont NM, Oudkerk JC, Dewael TY, Sadoun MJ. From artisanal to CAD-CAM blocks: state of the art of indirect composites. *J Dent Res* 2016;95:487–95.
- [15] Gracis S, Thompson VP, Ferencz JL, Silva NR, Bonfante EA. A new classification system for all-ceramic and ceramic-like restorative materials. *Int J Prosthodont* 2015;28:227–35.
- [16] Association AD, CDT: code on dental procedures and nomenclature 2015.
- [17] Callister Jr WD. *Materials science and engineering: an introduction*. 7th ed. New York: John Wiley & Sons; 2007.
- [18] Guess PC, Zavanelli RA, Silva NR, Bonfante EA, Coelho PG, Thompson VP. Monolithic CAD/CAM lithium disilicate versus veneered Y-TZP crowns: comparison of failure modes and reliability after fatigue. *Int J Prosthodont* 2010;23:434–42.
- [19] Wendler M, Belli R, Petschelt A, Mevec D, Harrer W, Lube T, et al. Chairside CAD/CAM materials. Part 2: flexural strength testing. *Dent Mater* 2017;33:99–109.
- [20] Horvath SD. Key parameters of hybrid materials for CAD/CAM-based restorative dentistry. *Compend Contin Educ Dent* 2016;37:638–43.
- [21] Elmougy A, Schiemann AM, Wood D, Pollington S, Martin N. Characterisation of machinable structural polymers in restorative dentistry. *Dent Mater* 2018;34:1509–17.
- [22] Menini M, Conserva E, Tealdo T, Bevilacqua M, Pera F, Signori A, et al. Shock absorption capacity of restorative materials for dental implant prostheses: an in vitro study. *Int J Prosthodont* 2013;26:549–56.
- [23] Conserva E, Menini M, Tealdo T, Bevilacqua M, Ravera G, Pera F, et al. The use of a masticatory robot to analyze the shock absorption capacity of different restorative materials for prosthetic implants: a preliminary report. *Int J Prosthodont* 2009;22:53–5.
- [24] Kaleli N, Sarac D, Kulunk S, Ozturk O. Effect of different restorative crown and customized abutment materials on stress distribution in single implants and peripheral bone: a three-dimensional finite element analysis study. *J Prosthet Dent* 2018;119:437–45.
- [25] Dogan DO, Gorler O, Mutaf B, Ozcan M, Eyuboglu GB, Ulgey M. Fracture resistance of molar crowns fabricated with monolithic all-ceramic CAD/CAM materials cemented on titanium abutments: an in vitro study. *J Prosthodont* 2017;26:309–14.
- [26] Kruzic JJ, Arsecularatne JA, Tanaka CB, Hoffman MJ, Cesar PF. Recent advances in understanding the fatigue and wear behavior of dental composites and ceramics. *J Mech Behav Biomed Mater* 2018;88:504–33.
- [27] Schlenz MA, Schmidt A, Rehmann P, Wostmann B. Fatigue damage of monolithic posterior computer aided designed/computer aided manufactured crowns. *J Prosthodont Res* 2019;63:368–73.
- [28] Zhang Y, Bhowmick S, Lawn B. Competing fracture modes in brittle materials subject to concentrated cyclic loading in liquid environments: monoliths. *J Mater Res* 2005;20:2021–9.
- [29] Zhang Y, Sailer I, Lawn BR. Fatigue of dental ceramics. *J Dent* 2013;41:1135–47.
- [30] Bonfante EA, Coelho PG. A critical perspective on mechanical testing of implants and prostheses. *Adv Dent Res* 2016;28:18–27.
- [31] Coelho PG, Jimbo R, Tovar N, Bonfante EA. Osseointegration: hierarchical designing encompassing the micrometer, micrometer, and nanometer length scales. *Dent Mater* 2015;31:37–52.
- [32] Bonfante EA, Suzuki M, Lorenzoni FC, Sena LA, Hirata R, Bonfante G, et al. Probability of survival of implant-supported metal ceramic and CAD/CAM resin nanoceramic crowns. *Dent Mater* 2015;31:e168–77.
- [33] Bonfante EA, Suzuki M, Hirata R, Bonfante G, Fardin VP, Coelho PG. Resin composite repair for implant-supported crowns. *J Biomed Mater Res B Appl Biomater* 2016;105(6):1481–9.
- [34] Nelson W. *Accelerated testing: statistical models, test plans and data analysis*. New York: John Wiley & Sons; 2004.
- [35] Coelho PG, Bonfante EA, Silva NR, Rekow ED, Thompson VP. Laboratory simulation of Y-TZP all-ceramic crown clinical failures. *J Dent Res* 2009;88:382–6.
- [36] Coelho PG, Silva NR, Bonfante EA, Guess PC, Rekow ED, Thompson VP. Fatigue testing of two porcelain-zirconia all-ceramic crown systems. *Dent Mater* 2009;25:1122–7.
- [37] Zhao WE, EA. A general accelerated life model for step-stress testing. *IIE Trans* 2005;37:1059–69.
- [38] Greaves GN, Greer AL, Lakes RS, Rouxel T. Poisson's ratio and modern materials. *Nat Mater* 2011;10:823–37.
- [39] Stocchero M, Jinno Y, Toia M, Jimbo R, Lee C, Yamaguchi S, et al. In silico multi-scale analysis of remodeling peri-implant cortical bone: a comparison of two types of bone structures following an undersized and non-undersized technique. *J Mech Behav Biomed Mater* 2020;103:103598.
- [40] van der Bilt A, Tekamp A, van der Glas H, Abbink J. Bite force and electromyography during maximum unilateral and bilateral clenching. *Eur J Oral Sci* 2008;116:217–22.
- [41] Ramos Nde C, Campos TM, Paz IS, Machado JP, Bottino MA, Cesar PF, et al. Microstructure characterization and SCG of newly engineered dental ceramics. *Dent Mater* 2016;32:870–8.
- [42] Swain MV, Coldea A, Bilkhair A, Guess PC. Interpenetrating network ceramic-resin composite dental restorative materials. *Dent Mater* 2016;32:34–42.
- [43] Della Bona A, Corazza PH, Zhang Y. Characterization of a polymer-infiltrated ceramic-network material. *Dent Mater* 2014;30:564–9.
- [44] Yamaguchi S, Kani R, Kawakami K, Tsuji M, Inoue S, Lee C, et al. Fatigue behavior and crack initiation of CAD/CAM resin composite molar crowns. *Dent Mater* 2018;34:1578–84.
- [45] Urdaneta RA, Marincola M, Weed M, Chuang SK. A screwless and cementless technique for the restoration of single-tooth implants: a retrospective cohort study. *J Prosthodont* 2008;17:562–71.
- [46] Verissimo AH, Duarte Moura DM, de Oliveira Dal Piva AM, Bottino MA, de Fatima Dantas de Almeida L, da Fonte Porto Carreiro A, et al. Effect of different repair methods on the bond strength of resin composite to CAD/CAM materials and microorganisms adhesion: an in situ study. *J Dent* 2020;93:103266.

- [47] Almeida EO, Freitas Jr AC, Bonfante EA, Marotta L, Silva NR, Coelho PG. Mechanical testing of implant-supported anterior crowns with different implant/abutment connections. *Int J Oral Maxillofac Implants* 2013;28:103–8.
- [48] Bozkaya D, Muftu S. Efficiency considerations for the purely tapered interference fit (TIF) abutments used in dental implants. *J Biomech Eng* 2004;126:393–401.